



STATIONARY HEAT TRANSFER AND AIRFLOW SIMULATION FOR TEST POLYGON HOUSES

J. Ratnieks, A. Jakovičs, S. Gendelis

*University of Latvia
Zellu street 8, LV-1002 – Latvia*

ABSTRACT

Energy efficiency of houses is highly topical problem nowadays, low energy consumption buildings are being built around the world, however, the thermal comfort is an issue that must be dealt with. For this purpose the test polygon of five houses with various construction solutions are being built in Riga, Latvia for which the aim is to acquire the best energy efficiency together with thermal comfort.

This work deals with stationary heat transfer and airflow simulations in test houses, the ANSYS/CFX software is used for the study. The modelling approach includes two model types. The first type is a 3D air region with heat transfer coefficient (third type) boundary conditions on outer surfaces to account for structures heat insulation. The second model type is a full 3D model including walls for lightweight plywood and rock wool construction. The heating is done with air to air heat pump and the room is being ventilated with an opening near the ceiling. The analyses are made for different velocities. The methodology for airflow and heat transfer simulations is developed and results are discussed.

Keywords: fluid dynamics, thermal comfort, energy efficiency

1. INTRODUCTION

The aim of this work is to develop a methodology to compute airflow and thermal behaviour of different building structures, taking into account humidity, rain and thermal radiation. The equations governing airflow are nonlinear and difficult to solve and usually numerically unstable, therefore the thermal radiation and humidity is left for further studies and heat exchange due to transmission and convection are studied. The second section deals with the experimental test polygon built in Riga with description of constructions used and methodology described. Two different modelling strategies are being studied the first being only the fluid domain with solid domain replaced with boundary conditions and the second include also the real thickness and material properties of the solid domains. The modelling approach, assumptions used and implementation in ANSYS/CFX as well as governing equations and meshing are described in section three: “mathematical model”. Sections four and five are results and discussion respectively.

2. EXPERIMENTAL SETUP

The project within which this particular research is done deals with both – energy efficiency of different building constructions made in Latvia, suitable for local climate conditions [1], and ensuring A class thermal comfort criteria defined by [2]. To achieve the aim all the available construction solutions were identified and five building structures that appeared to be sustainable were set up in Riga (Fig.1). These constructions include lightweight constructions with small thermal inertia and massive constructions with high thermal inertia. Also the life cycled for each construction type differs. the wooden log and rock wool construction (LOG); plywood, rock wool and fibrolite construction (PLY); clay brick wall with rock wool insulation layer (CER); lightweight aerated concrete with rock wool insulation layer (AER) and innovative clay brick construction where macroscopic holes are filled with insulating material to avoid convection in them (EXP) (Fig. 2). The thermal transmittance for all cases for walls are $U=0.16 \text{ W/m}^2\text{K}$. For doors and windows thermal transmittance is $U=1 \text{ W/m}^2\text{K}$, so the heat losses through them will be higher. For

every structure there are air – air heat pump installed and total energy consumption is measured throughout the year including both heating and cooling. For periods of time when the construction is not available to keep the thermal comfort conditions there is a penalty function introduced.

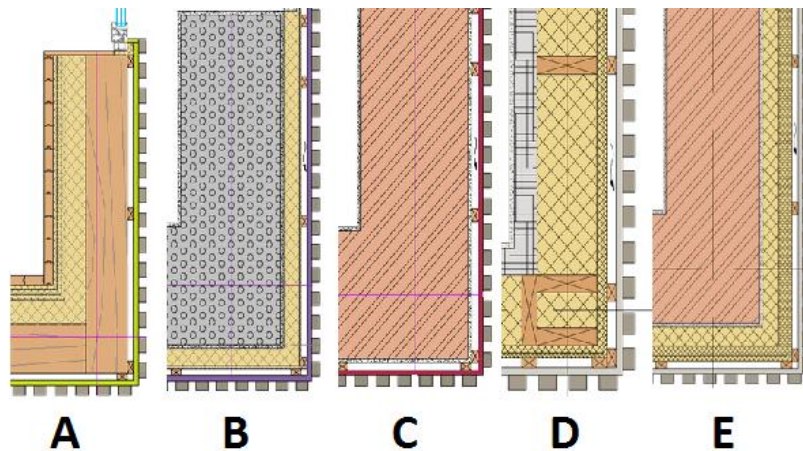


Fig. 1. Different construction types used in the project: a) LOG, b) AER, c) EXP, d) PLY, e) CER



Fig. 2. Test polygon at building stage on the left and finished stage on the right

3. MATHEMATICAL MODEL

3.1. Modelling approach

Two different cases are being considered in this work. As the roof is not being heated, it is removed from the mathematical model and heat losses through ceiling are computed as there was no roof construction present. As the thermal transmittivity is equal for all cases a good approximation would be to exclude the walls from the model and replace them with boundary conditions (Fig. 3a). Third type boundary conditions are suitable for modelling as the outside temperature can be adjusted and thermal transmittivity can be modelled by setting the correct heat transfer coefficient value. The downside of this method is that thermal capacity is not taken into account that is important for time dependent simulations as the outside weather conditions change rapidly, however it gives a good limit of what happens when there is no thermal inertia in the construction.

The second approach is to use a model with walls included (Fig. 3b) and material properties defined properly. This kind of approach is needed to correctly predict thermal behaviour of construction during daily cycles and reaction to sudden outside conditions. For this particular case the plywood is removed to avoid thin regions, but its influence is taken into account by changing material properties for rock wool and fibrolite, the thermal conductivity is higher for the latter. The rock wool is on the outside (cold side) and fibrolite on inside (Fig. 1d).

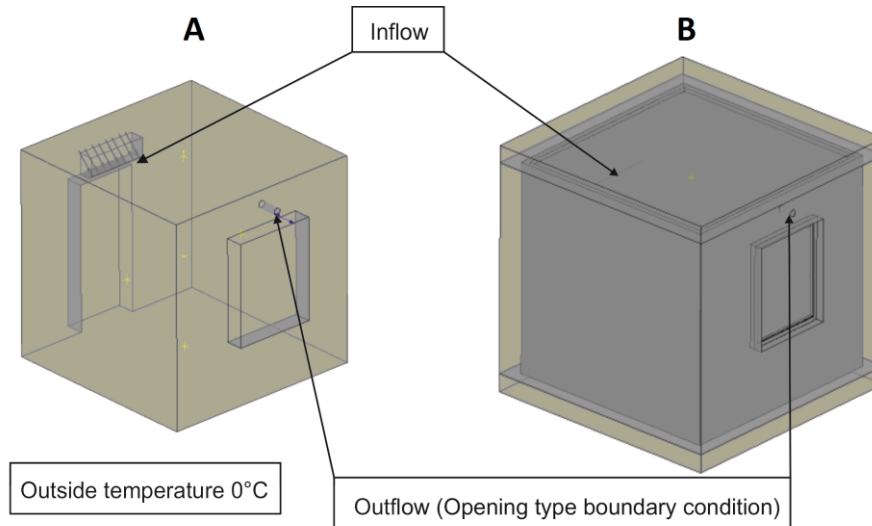


Fig. 3. Mathematical models: a) concentrated thermal resistance model b) full walls model

An issue for computational fluid dynamics (CFD) has always been validity of results. For many other physics equations there are analytic solutions that help to determine the correctness of numerical solutions. In CFD the only analytic solution is a Poiseuille flow in an infinite tube that is not valid in this study, so the only verification is by experiment. As the experimental results are not available yet the validation will be made by calculation of thermal balance and evaluating symmetry of the problem. There are also five monitor points in the model to see the development of temperature and velocity fields. They are marked with yellow labels (Fig. 3) two are equidistant from symmetry plane.

3.2. Governing equations and implementation in ANSYS/CFX

The Reynolds averaged Navier Stokes (RANS) equations are used for conservation of momentum along with energy conservation equation and continuity equation [3, 4, 5]. To model the buoyancy the Boussinesq approximation [3, 4] is used in which the density is assumed constant and the body force is temperature dependent. The temperature is taken from heat transfer equation.

Typically the airflow in a room is turbulent and it can easily be shown (Eq. 1) by Reynolds number that characterize the flow. As the characteristic length can be chosen 1.5 m, density is 1.225 kg/m^3 and dynamic viscosity $1.983 \cdot 10^{-5} \text{ kg/s}\cdot\text{m}$ the velocity, at which Reynolds number exceed 2000 that is typical value when flow become turbulent, is 1.1 cm/s

$$\text{Re} = \frac{\rho \cdot L \cdot v}{\mu} \quad (1)$$

where ρ – density, L – characteristic length, v – velocity and μ – dynamic viscosity.

The $k-\omega$ shear stress transport (SST) turbulence model is used that is built-in ANSYS/CFX software [3, 4]. This turbulence model was chosen because it is two parameter model that has the best performing parts of $k-\omega$ and $k-\epsilon$ turbulence models [4].

3.3. Boundary conditions

To model the source an inlet boundary condition was used for which the inflow air velocity and direction need to be provided in this case the velocities are 0.1 m/s, 0.2 m/s and 0.3 m/s and at all cases the inflow temperature is constant $T=25^\circ\text{C}$. The other options involved the mass flow and pressure difference, but as the Boussinesq approximation keep the density constant over the domain the post-processing is easier with the velocity approach. For mass sink there was an opening type

boundary condition to perfectly balance the mass inside domain as it was the only mass sink available in the model.

For the concentrated thermal resistance case the third type boundary conditions were used to model the thermal resistance of the wall and natural convection. The outside temperature were set to 0°C and the heat transfer coefficient was calculated (eq. 2) taking into account convection and thermal resistance of the wall [5].

$$U = \frac{1}{R_{wall} + R_{convOut}} \quad (2)$$

Where U – heat transfer coefficient [$W/(m^2K)$], R_{wall} – thermal resistance of the wall, $R_{convOut}$ – thermal resistance due to convection on the outside boundary. As example, the thermal resistance of wall is $R_{wall}=1/U=6.25$ [m^2K/W] and $R_{convOut}=0.04$ [m^2K/W].

For the full wall model the outer wall boundary condition is first term on the right side disappear and the heat transfer coefficient accounts only for natural convection.

The fluid solid boundaries for fluid flow are modelled as no slip walls.

3.4. Meshing

For both cases maximum mesh size for fluid domains were 4 cm and for the full wall model the maximum mesh size was 5 cm for solid domains. For mass source and sink regions the mesh was made smaller by using sphere of influence at the sink and at the source to get the mesh resolution below 1 cm. The inflation was used on the walls with 5 boundary layers all over the domain except for source and sink boundaries.

4. RESULTS

4.1. Concentrated thermal resistance model

First calculations were made with the concentrated thermal resistivity model, the convergence criteria were set to 10^{-4} that it never reached, but after 3000 iterations the solution started to oscillate around certain value. The thermal balance acquired was below 0.4% off that is good for CFD simulations. However the model had noticeable asymmetry (Fig. 4). Further study was to make time-dependent calculations after the asymmetric result was achieved. This approach gave more symmetrical results, but for larger time steps the thermal balance diverged and more heat was leaving the system then was pumped in.

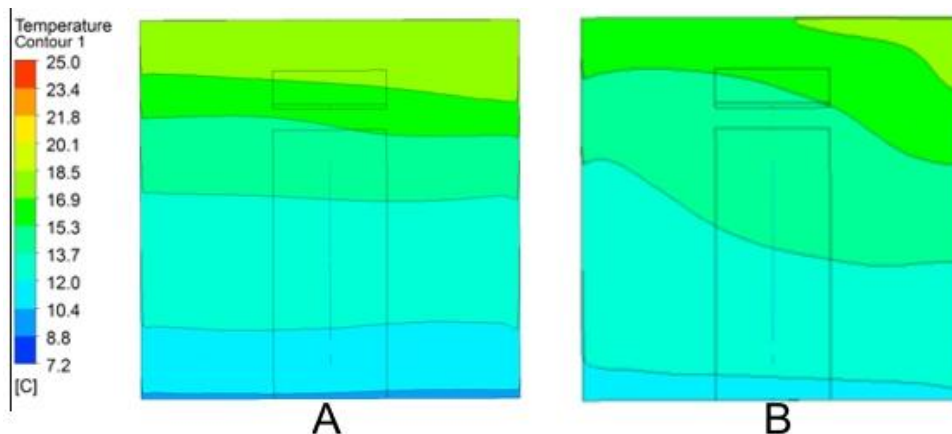


Fig. 4. Concentrated thermal resistance model a) Time-dependent solution after 120 seconds with time step 0.1 s b) stationary solution

As this model had limitations on further studies because of thermal inertia and the full model showed more numerical stability the former was discarded and only the latter was studied.

4.2. Full wall model

Studies with full wall model had previous asymmetry for large number of stationary iterations and time-dependent analysis took considerable computational time to achieve symmetrical velocities and temperature profiles. The studies showed that by choosing good initial temperature guess after 100 iterations (Fig. 5a) the thermal balance was fine, as showed later. For time dependent simulation (Fig. 5b) seemingly stationary solution was acquired after 4 minutes of simulation time (Fig. 6) with time steps being 0.1 s.

The calculations were made for three different cases with velocities being 0.1 m/s, 0.2 m/s and 0.3 m/s. The former is a boundary case with air exchange of 0.6 h⁻¹ as planned for experiment. This shows that feedback to air pump is necessary to keep the inside temperature habitable. The velocity profile for 0.3 m/s simulation is shown in Fig. 5.

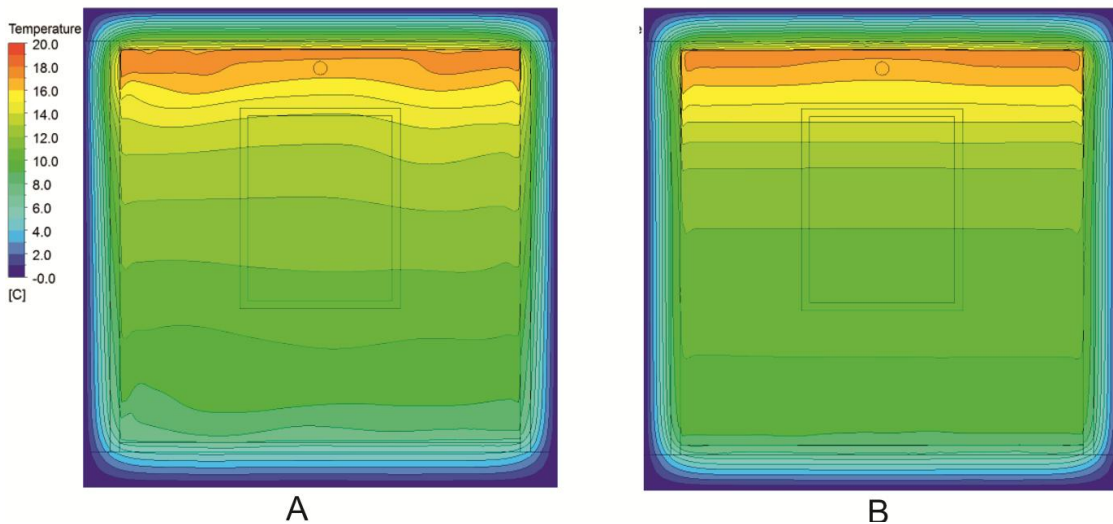


Fig. 5. Temperature fields for inflow velocity 0.3 m/s for a) stationary solution
 b) time-dependent solution

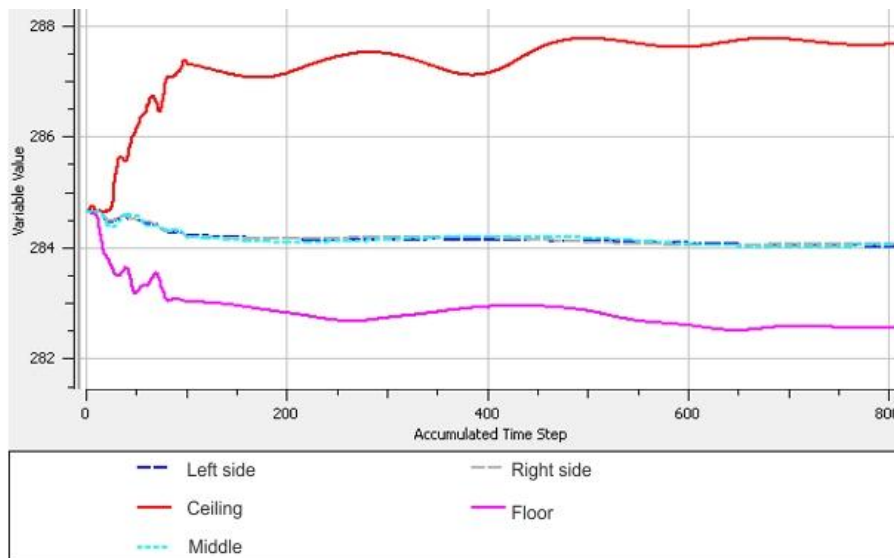


Fig. 6. Monitor point temperature values for each stationary iteration for stationary run and timestep for transient run (inflow velocity 0.2 m/s)

Heat balance calculations were carried out after 100 iterations of stationary solver and initial temperature adjusted to reduce heat balance error. When satisfactory result was obtained, time-dependent solver was run and thermal balance calculated once more (Table 1).

For walls, ceiling, floor, window and doors the heat losses were computed as area integral of heat flux (Eq. 3). At the mass sources and sinks (ventilation and heat pump (table 1)) velocity and temperature were integrated over the surface (eq.4)

$$P_{\phi} = \int_s \vec{\Phi} d\vec{S} \quad (3)$$

$$P_j = C_p \rho \int_s T \vec{v} d\vec{S} \quad (4)$$

Where P_{ϕ} – heat losses through solids [W], Φ – heat flux [W/m^2], C_p – specific heat at constant pressure [$\text{J}/(\text{kgK})$]; ρ – density [kg/m^3], T – temperature [K], v – velocity [m/s].

Table 1. Heat balance for various inflow velocities for the full wall model for time-dependent solver run with stationary solution initial values

Inlet velocity, m/s	0.1	0.2	0.3
heat losses, W			
walls	-40.89744	-54.2686	-60.0715
door	-9.34263	-12.9553	-14.005
window	-9.08604	-11.8835	-13.6166
ceiling	-19.11222	-24.4689	-27.6394
floor	-9.60057	-11.8228	-16.255
ventilation	-61.55	-141.18	-253.78
total	-149.5889	-256.5791	-385.3675
heat gain, W			
heat pump	132.19	262.29	390.91
difference, W	-17.3989	5.7109	5.5425
error, %	13.2	2.2	1.4

The heat losses through construction elements are higher with high inflow velocities. This is reasonable because the overall temperature in the model is higher and therefore temperature difference between inside and outside. Heat loss through ceiling is higher than loss through floor for the temperature differences. The heat gain is proportional the inflow speed as it should be but the ventilation losses differ because the outlet temperature can vary as it does.

5. DISCUSSION

Although the experimental verification is not yet unavailable this would not help to verify model yet because the solar influence and humidity is not taken into account. At this point it is possible only to make some qualitative remarks on the solution. First of all the authors would like to point out that velocity vectors near the doors and window are directed toward the floor that is physically expected as the temperature near these regions is low (Fig. 7), also the hot air near the inflow is rising that gives that proves that the buoyancy is working correctly (Fig. 8).

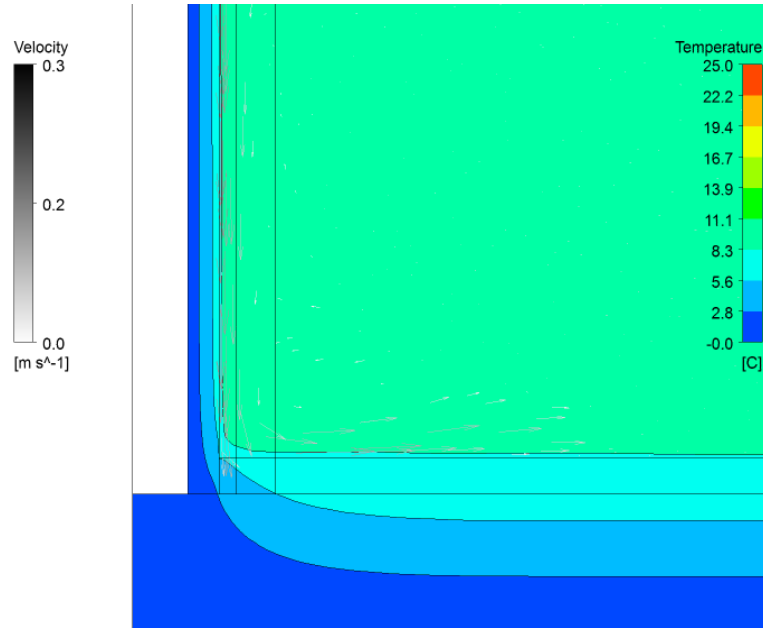


Fig. 7. Temperature field and velocity vectors near the doors region

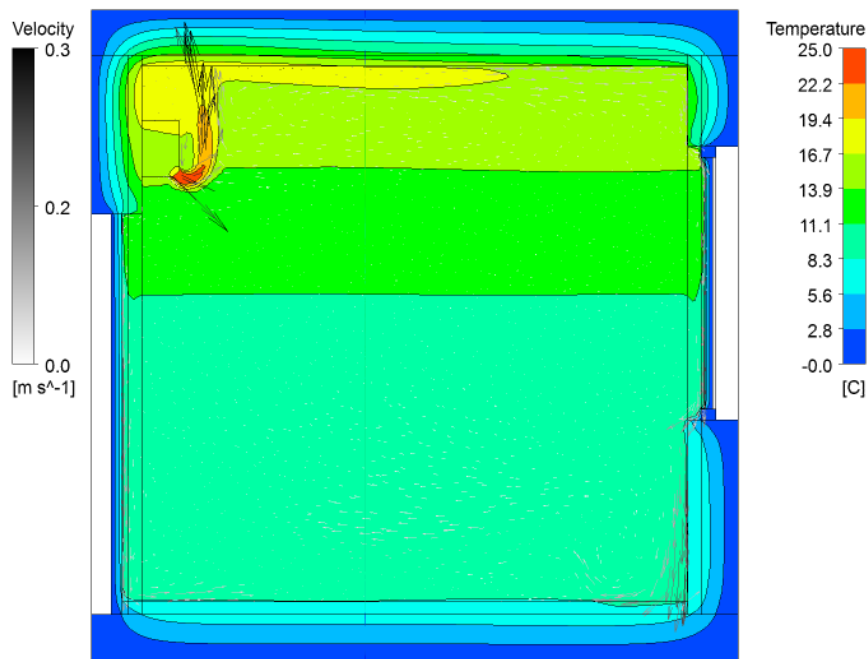


Fig. 8. Temperature field and velocity vectors on plane near the symmetry plane

As previously mentioned the thermal conductivity coefficient for rock wool is smaller than for fibrolite. The isotherms on the rock wool layer are closer to each other that mean the temperature gradient there is higher (Fig. 9).

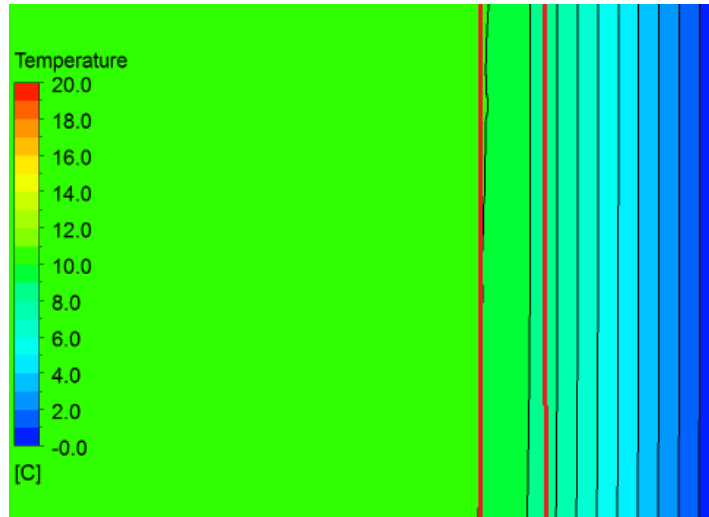


Fig. 9. Isotherms on the solid cross section (domain boundaries are marked with red)

6. CONCLUSION AND FURTHER STUDIES

Stationary solution for both problems gives unphysical results for given mesh and therefore a methodology that involve time-dependent calculations have been developed. The results have been qualitatively analyzed using symmetry and thermal balance and no physical inconsistency have been found that proves the methodology developed is useful for this kind of simulations.

Further work will concentrate on the thermal radiation implementation in the model and humidity impact on results will be considered. The feedback to heat pump will be included in the model to increase the inlet velocity to get inhabitable temperature distribution in room. Empirical observations have indicated that 0.6 m/s is enough.

7. ACKNOWLEDGEMENT

This work has been supported by the European Regional Development Fund in Latvia, project Nr. 2011/0003/2DP/2.1.1.1.0/10/APIA/VIAA/041.

8. REFERENCES

1. OZOLINS Ansis, JAKOVICS Andris, Heat and moisture transport in multi layer walls interaction and heat loss at varying outdoor temperatures, 2012, Latvian Journal of Physics and Technical Sciences, N6(I), p. 32–43
2. LVS EN ISO 7730, Ergonomics of the thermal environment – Analytical determination and interperatation of thermal comfort using calculation of the PMV and PPD indices and local thermal comfort criteria, 2006, third ed.
3. ANSYS Inc., Ansys CFX solver theory guide, 2011.
4. MENTER, FLORIAN R., Two-equation eddy-viscosity turbulence models for engineering applications, *AIAA-Journal*, 1994, Vol. 32(8), p. 1598 – 1605.
5. GENDELIS, STANĪSLAVS, Complex analysis of thermophysical processes in buildings, 2012, University of Latvia, PhD Theses.